Distributions of Distances and Volumes of Balls in Homogeneous Lens Spaces

Brenden Balch, Chris Peterson, and Clayton Shonkwiler

Department of Mathematics, Colorado State University, Fort Collins, CO

Abstract

Lens spaces are a family of manifolds that have been a source of many interesting phenomena in topology and differential geometry. Their concrete construction, as quotients of odd-dimensional spheres by a free linear action of a finite cyclic group, allows a deeper analysis of their structure. In this paper, we consider the *problem of moments* for the distance function between randomly selected pairs of points on homogeneous three-dimensional lens spaces. We give a derivation of a recursion relation for the moments, a formula for the $k^{\rm th}$ moment, and a formula for the moment generating function, as well as an explicit formula for the volume of balls of all radii in these lens spaces.

1 Introduction

Given a set of data, what is the best guess for the random process that produced the data? Attempts to answer special cases of this question have motivated new developments in statistics, mathematics, and machine learning. As a starting point, one would like to understand whether the observed data has a distribution differing from what is "expected." However, determining what is expected can be quite subtle when the data takes values on a manifold, though when the manifold is homogeneous, there are additional tools that one can use to simplify the problem. At an intuitive level, a homogeneous manifold is a space in which each point is indistinguishable from any other point.

For distance data, one would ideally like to check whether the distribution of pairwise distances is compatible with the corresponding distribution on the manifold. In a previous paper [4], we considered the problem of computing the expected distances between randomly drawn points on manifolds of partially oriented flags. These manifolds generalize projective spaces and other Grassmannians and form a large family of homogeneous spaces. The examples in which we had the most success computing expected distances turn out to be

(scaled) lens spaces; that is, quotients of an odd-dimensional sphere by the free action of a cyclic group. In this paper we go beyond simple expectations and determine precisely the distributions of distances between pairs of random points in all homogeneous three-dimensional lens spaces.

These distributions are examples of distance distributions (or sometimes shape distributions or distance histograms), which make sense on arbitrary metric measure spaces, and are often used for geometric classification and shape analysis [5, 6, 7, 8, 17, 18, 19]. Our results provide a strong statistical baseline against which to compare data on lens spaces, which have recently been applied to data science [20], appear frequently in the cosmography literature [1, 3, 26, 27], and are the natural setting for spherical data with cyclic symmetries.

To establish notation, each pair of positive integers (n, m) with n > m and gcd(n, m) = 1 determines a three-dimensional lens space L(n; m) which is a quotient of the 3-sphere \mathbb{S}^3 by the cyclic group of order n. By requiring the quotient to be a Riemannian submersion, we induce a Riemannian metric on L(n; m), which turns out to be homogeneous when m = 1 or n-1. Moreover, L(n; 1) and L(n; n-1) are isometric, so to understand distance distributions on homogeneous lens spaces it suffices to consider those lens spaces of the form L(n; 1).

As a first step, we determine all moments of distance (i.e., expected values of powers of distance) by solving a recurrence relation that they satisfy:

Theorem 1. For each $k \geq 0$ and each $n \geq 2$, the kth moment of distance on L(n; 1) is

$$I_{n,k} = \frac{1}{(k+1)(k+2)} \left[\frac{4}{k+3} \left(\frac{\pi}{n} \right)^{k+2} {}_{1}F_{2} \left[\frac{1}{\frac{k+4}{2}, \frac{k+5}{2}}; -\frac{\pi^{2}}{n^{2}} \right] + \tan \frac{\pi}{n} \left(n \left(\frac{\pi}{2} \right)^{k+1} {}_{1}F_{2} \left[\frac{1}{\frac{k+3}{2}, \frac{k+4}{2}}; -\frac{\pi^{2}}{4} \right] - 2 \left(\frac{\pi}{n} \right)^{k+1} {}_{1}F_{2} \left[\frac{1}{\frac{k+3}{2}, \frac{k+4}{2}}; -\frac{\pi^{2}}{n^{2}} \right] \right) \right],$$

where for n=2 this is interpreted as the limit of the above expression as $n \to 2$, and $_1F_2$ is a hypergeometric function whose definition we recall on page 9 below.

The alternating finite sum formula given in (8) is typically more useful for small k, but one virtue of this formulation in terms of hypergeometric functions is that it is easy to extract asymptotic information:

Corollary 2. As $k \to \infty$ the kth moment of distance grows like

$$I_{2,k} \sim \frac{2}{k} \left(\frac{\pi}{2}\right)^k$$
 and $I_{n,k} \sim \frac{n}{k^2} \left(\frac{\pi}{2}\right)^{k+1} \tan \frac{\pi}{n}$ for $n \ge 3$.

A more attractive and systematic packaging of the moments is in the form of the moment-generating function of distance:

Theorem 3. The moment-generating function of distance on L(n; 1) is

$$M_n(t) = \begin{cases} \frac{4}{\pi(4+t^2)} \left(\frac{2(e^{t\pi/2}-1)}{t} + te^{t\pi/2} \right) & \text{if } n = 2\\ \frac{2n}{\pi(4+t^2)} \left(\frac{2(e^{t\pi/n}-1)}{t} + \tan\frac{\pi}{n} \left(e^{t\pi/2} - e^{t\pi/n} \right) \right) & \text{if } n \ge 3. \end{cases}$$

We then use the moment-generating function to determine the cumulative distribution function of distance, which (up to scaling) simply reports volumes of balls. Consequently, our probabilistic approach to studying distances on lens spaces yields the following purely geometric result:

Theorem 4. For $n \geq 2$, the volume of a ball of radius r in L(n;1) is

$$V_n(r) = \begin{cases} 2\pi(r - \sin r \cos r) & \text{if } r \le \frac{\pi}{n} \\ \frac{2\pi^2}{n} - 2\pi \cos^2 r \tan \frac{\pi}{n} & \text{else.} \end{cases}$$

Notice, in particular, that this formula for volume extends beyond the injectivity radius $\frac{\pi}{n}$ of L(n;1), in contrast to most results about volumes of balls in Riemannian manifolds (e.g., [14]). In addition to the potential applications of these ideas to data problems, this seems to be a novel result to add to existing knowledge about the geometry and topology of lens spaces [2, 9, 15, 16, 21, 22, 23, 24, 28].

We describe our perspective, provide basic background material on lens spaces, and give the setting in which algorithms and analytic computations are to be made in Section 2. In Section 3 we describe algorithms for sampling random points and determining their distance apart. In addition, we present the results of several Monte Carlo experiments that illustrate differences between distributions of distances on homogeneous and non-homogeneous lens spaces. Section 4 contains the main theoretical results of the paper.

2 Lens Spaces

Three-dimensional lens spaces are a family of manifolds that arise as the orbit space of a finite cyclic group acting freely on the unit 3-sphere. More precisely, let $Z_n = \{e^{i2\pi k/n} \in \mathbb{C} \mid 1 \le k \le n\}$ denote the cyclic group of order n and consider $\mathbb{S}^3 = \{(\alpha, \beta) \in \mathbb{C}^2 \mid |\alpha|^2 + |\beta|^2 = 1\}$. Given $n, m \in \mathbb{N}$ with $\gcd(m, n) = 1$, there is a free action of Z_n on \mathbb{S}^3 defined by

$$\omega \cdot (\alpha, \beta) = (\omega \alpha, \omega^m \beta),$$

for each $\omega \in \mathbb{Z}_n$. The resulting orbit space is the lens space L(n; m).

To visualize L(n; m), we can look at the fundamental domain of the Z_n action on $\mathbb{S}^3 \subseteq \mathbb{C}^2$, as in Figure 1. The fundamental domain of the rotation $e^{2\pi i/n}$ in the first factor is an arc of length $\frac{2\pi}{n}$ in the unit circle in the z_1 -plane of \mathbb{C}^2 . All points in \mathbb{S}^3 with first coordinate in such a fundamental domain form a lens-shaped domain as pictured. The top and bottom faces of the lens consist of all points lying on geodesics connecting an endpoint of the arc to all points in the unit circle in the z_2 -plane: these are hemispheres of unit 2-spheres meeting at an angle of $\frac{2\pi}{n}$ along the unit circle in the z_2 -plane. Since the endpoints of the arc are identified under the $\frac{2\pi}{n}$ rotation in the z_1 -coordinate, the bottom face is identified with the top face by this rotation. However, this identification happens with a $\frac{2\pi m}{n}$ twist in the z_2 -coordinate, so that the green sector in the bottom face is glued to the green sector in the top face (in the picture, m=2).

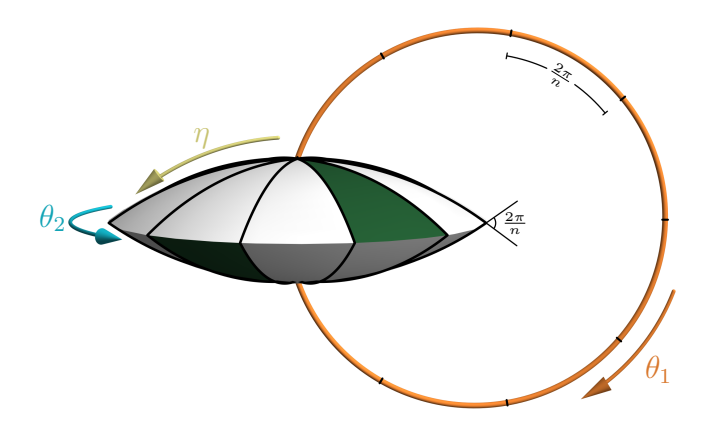


Figure 1: A fundamental domain of the lens space L(n; m). The arrows indicate the directions of the join coordinates $(\theta_1, \theta_2, \eta)$ that will be defined on page 5.

Lens spaces were introduced by Tietze [25] and have historically provided interesting examples of manifolds which cannot be distinguished by homology or homotopy groups. For example, L(5;1) and L(5;2) are not homeomorphic (nor even homotopy equivalent) despite the fact that $\pi_1(L(5;1)) \cong \pi_1(L(5;2))$ and $H_{\bullet}(L(5;1)) \cong H_{\bullet}(L(5;2))$ [2]. In fact, the lens spaces $L(n;m_1)$ and $L(n;m_2)$ are homotopy equivalent if and only if $m_1m_2 = \pm a^2 \pmod{n}$ for some $a \in \mathbb{N}$, and are homeomorphic if and only if $m_1 = \pm m_2^{\pm 1} \pmod{n}$ [9, 22]. Using these criteria, one can easily conclude that L(7;1) and L(7;2) are examples of manifolds which are homotopy equivalent but not homeomorphic.

In addition to their topological structure, lens spaces have geometric structure. The round metric on \mathbb{S}^3 induces a unique metric on $\mathbb{S}^3/Z_n = L(n;m)$ that makes $\pi: \mathbb{S}^3 \to L(n;m)$ a Riemannian submersion. A result of Ikeda and Yamamoto [15] implies that two three-dimensional lens spaces are isometric if and only if they are homeomorphic. This result, combined with work of Tanaka [24], shows that the spectrum of the Laplacian uniquely determines a three-dimensional lens space among all Riemannian manifolds. An explicit orthonormal eigenbasis for the Laplacian is given in [16]. Moreover, the isoperimetric problem has been solved in all lens spaces L(n;m) with n large enough [28].

With respect to this Riemannian metric, some lens spaces are homogeneous, meaning the isometry group acts transitively. Theorem 7.6.6 of Wolf [29] says that \mathbb{S}^d/G is homogeneous if and only if the group G has a Clifford representation—that is, a faithful orthogonal representation $\rho: G \to O(d+1)$ such that $\rho(g) = \pm I$ or half of the eigenvalues of $\rho(g)$ are $\lambda \in \mathbb{S}^1$ and the other half are $\bar{\lambda}$. The action of Z_n on \mathbb{S}^3 has the faithful orthogonal representation $\rho: Z_n \to O(4)$ given by

$$\rho(\omega) = \begin{pmatrix} \cos 2\pi/n & -\sin 2\pi/n & 0 & 0\\ \sin 2\pi/n & \cos 2\pi/n & 0 & 0\\ 0 & 0 & \cos 2\pi m/n & -\sin 2\pi m/n\\ 0 & 0 & \sin 2\pi m/n & \cos 2\pi m/n \end{pmatrix},$$

and has eigenvalues $e^{i2\pi/n}$, $e^{-i2\pi/n}$, $e^{i2\pi m/n}$ and $e^{-i2\pi m/n}$. Hence L(n;m) is homogeneous pre-

cisely when m = 1 or m = n - 1. Since L(n; 1) and L(n; n - 1) are homeomorphic and hence isometric, we may simply take m = 1 when dealing with homogeneous lens spaces.

2.1 Coordinate systems

Using the natural group structure on \mathbb{S}^3 given by its identification with the unit quaternions, we can describe an isomorphism between \mathbb{S}^3 and SU(2). Writing quaternions in the form $\alpha + \beta \mathbf{j}$ for $\alpha, \beta \in \mathbb{C}$, define $\varphi : \mathbb{S}^3 \to SU(2)$ by

$$\varphi: \alpha + \beta \mathbf{j} \mapsto \begin{pmatrix} \alpha & -\beta \\ \overline{\beta} & \overline{\alpha} \end{pmatrix},$$

where $\overline{\zeta}$ denotes the complex conjugate of ζ . It is easy to check that φ is a Lie group isomorphism. The action of Z_n on \mathbb{S}^3 then induces an action on SU(2) given explicitly by

$$\omega \cdot \begin{pmatrix} \alpha & -\beta \\ \overline{\beta} & \overline{\alpha} \end{pmatrix} = \begin{pmatrix} \omega \alpha & -\omega^m \beta \\ \overline{\omega^m \beta} & \overline{\omega \alpha} \end{pmatrix}. \tag{1}$$

Describing the lens space in this way will make our computations straightforward. The idea is that we can easily generate random elements of SU(2) according to Haar measure (which corresponds to the uniform probability measure on \mathbb{S}^3), compute the orbits explicitly, and then distances between orbits correspond to distances in the lens space.

For homogeneous lens spaces, we will be able to make explicit analytic calculations in Section 4. To do so, we'll parametrize \mathbb{S}^3 using *join coordinates*, which realize the 3-sphere as the join of two circles. Since $\mathbb{S}^3 = \{(\alpha, \beta) \in \mathbb{C}^2 \mid |\alpha|^2 + |\beta|^2 = 1\}$, we can write $\alpha = e^{i\theta_1} \cos \eta$ and $\beta = e^{i\theta_2} \sin \eta$ for $\theta_1, \theta_2 \in [-\pi, \pi)$ and $\eta \in [0, \pi/2]$. This can also be expressed in Cartesian coordinates on \mathbb{R}^4 as

$$x = \cos \theta_1 \cos \eta$$

$$y = \sin \theta_1 \cos \eta$$

$$z = \cos \theta_2 \sin \eta$$

$$w = \sin \theta_2 \sin \eta.$$
(2)

These coordinates easily yield the volume form $d\text{Vol}_{\mathbb{S}^3} = \cos \eta \sin \eta \, d\eta \wedge d\theta_1 \wedge d\theta_2$, and the volume form induced by the Riemannian submersion metric on the homogeneous lens space L(n;1) is $d\text{Vol}_{L(n;1)} = \cos \eta \sin \eta \, d\eta \wedge d\theta_1 \wedge d\theta_2$, where now $\theta_1, \theta_2 \in [-\pi/n, \pi/n)$. A straightforward calculation shows that $\text{Vol}(L(n;1)) = 2\pi^2/n^2$.

3 Algorithms and Experiments

In this section we'll provide an algorithm for a Monte Carlo experiment. We then use this as a guide for analysis on higher moments.

Algorithm 1 Random Special Unitary Matrix

```
1: function RANDSU(n)

2: A, B \leftarrow \text{random } n \times n \text{ Gaussian}

3: C \leftarrow A + iB \triangleright where i = \sqrt{-1}

4: Q \leftarrow \text{GRAMSCHMIDT}(C)

5: Q_{1,n} \leftarrow \frac{1}{\det(Q)}Q_{1,n} \triangleright Q_{1,n} is the last column of Q

6: end function
```

Our aim is to describe a Monte Carlo simulation which will allow us to approximate expected (Riemannian) distances between two points in L(n; m). We will use Algorithm 1 to randomly generate elements of SU(n).

We will use the Riemannian distance function on SU(2) (see [10]), then use the Riemannian submersion $\pi: SU(2) \to L(n;m)$ to obtain a distance function on the lens space. Suppose that $A, B \in SU(2)$, and let λ_1, λ_2 be the eigenvalues of AB^* . For a nonzero complex number z = x + yi, we let $\log z$ denote the principal value logarithm whose imaginary part lies in the interval $(-\pi, \pi]$. We have

$$d(A, B) = \frac{1}{\sqrt{2}} \sqrt{|\log \lambda_1|^2 + |\log \lambda_2|^2}$$

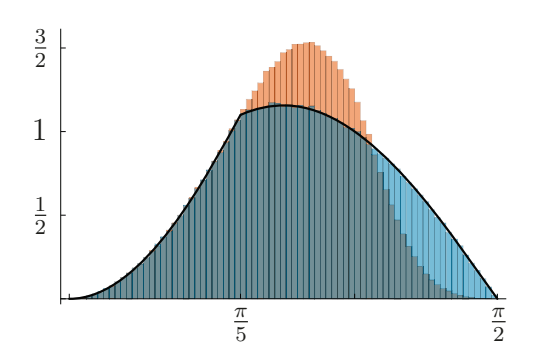
or, since $\lambda_2 = \overline{\lambda}_1$, $d(A, B) = |\log \lambda_1|$. To compute distances on L(n; m), we first compute the orbits, then compute pairwise distances between the elements of each orbit, and finally take the minimum of all distances computed. Thus for $[A], [B] \in L(n; m)$, we have

$$d([A], [B]) = \min_{1 \le j, k \le n} \{ d(\omega^j \cdot A, \omega^k \cdot B) \},$$

where $\omega = e^{2\pi i/n}$. This leads to Algorithm 2.

Algorithm 2 Expected Distance on L(n; m)

```
\triangleright Begin with a list of N zeroes
 1: D \leftarrow [0] * N
 2: for k \leftarrow 1, N do
           A \leftarrow \text{RANDSU}(2)
 3:
           B \leftarrow \text{RandSU}(2)
           orbitdata \leftarrow [0] * n \times n
                                                                                               \triangleright Initialize n \times n zero matrix
 5:
           for i \leftarrow 1, n do
 6:
                for j \leftarrow 1, n do
 7:
                     orbitdata(i, j) \leftarrow d(\omega^i \cdot A, \omega^j \cdot B)
 8:
                end for
 9:
           end for
10:
           D(k) \leftarrow \text{MIN}(\text{orbitdata})
11:
12: end for
return MEAN(D)
```



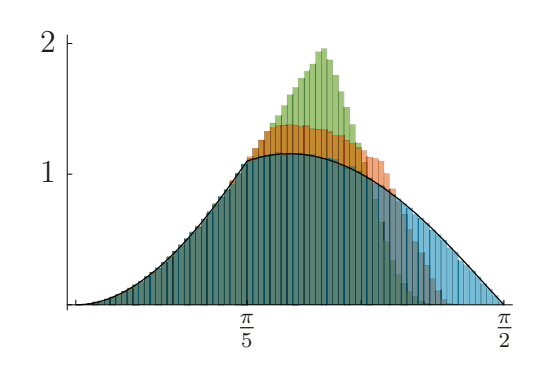


Figure 2: On the left are histograms of distances between 1,000,000 random pairs of points in L(5;1) [blue] and L(5;2) [red], computed using Algorithm 2; the curve shows the true density of distances in L(5;1) from (11). The right shows histograms of distances in L(5;2) from 1,000,000 random points to different fixed points, where the fixed points are the images in L(5;2) of SU(2) elements of the form $\begin{pmatrix} \cos \phi & -\sin \phi \\ \sin \phi & \cos \phi \end{pmatrix}$, where $\phi = 0$ [blue], $\pi/8$ [red], and $\pi/4$ [green]; the curve shows the density of distances from random points in L(5;1) to any fixed point, again from (11). In particular, whereas the distributions of distances from random points to any fixed point in the homogeneous space L(5;1) are all the same, these distributions vary with the fixed point in the non-homogeneous L(5;2).

For example, using Algorithm 2 with N=1,000,000, we estimate the expected distances between random points on L(5;1) and L(5;2) to be approximately 0.85897 and 0.80378, respectively, reflecting the fact that these lens spaces are not isometric (nor even homeomorphic); see Figure 2. The corresponding estimates for L(7;1) and L(7;2) are 0.82641 and 0.73641, respectively, again reflecting the fact that these spaces are neither isometric nor homeomorphic, though they are homotopy equivalent.

In the homogeneous case, it actually suffices to fix a representative of a fixed orbit, then check the distances between the chosen representative and each element of the other orbit. To see this, note that

$$d([A], [B]) = \min_{1 \le i, j \le n} \{ d(\omega^i \cdot A, \omega^j \cdot B)$$

=
$$\min_{1 \le k \le n} \{ d(\omega^k \cdot AB^*, I).$$

If A, B are chosen according to Haar measure on SU(2), then AB^* will also be distributed according to Haar measure, which is definitionally invariant under the (left or right) action of SU(2) on itself. Hence, when doing a computational experiment, we can generate one random element of SU(2), compute the orbit under the action, and then compute the distances from each element in the orbit to the identity. This yields the less computationally expensive Algorithm 3.

For N=1,000,000, a naïve Matlab implementation of Algorithm 2 gives the estimate $E[d;L(5,1)]\approx 0.85897$ in about 940 seconds on a laptop, whereas Algorithm 3 yields $E[d;L(5,1)]\approx 0.85921$ in about 86 seconds.

Algorithm 3 Expected Distance on L(n; 1)

```
1: D \leftarrow [0] * N

2: for l \leftarrow 1, N do

3: A \leftarrow \text{RANDSU}(2)

4: orbitdata \leftarrow [0] * n

5: for k \leftarrow 1, n do

6: orbitdata(k) \leftarrow d(\omega^k \cdot A, I)

7: end for

8: D(l) \leftarrow \text{MIN}(\text{orbitdata})

9: end for

return MEAN(D)
```

4 Distributions of Distances

We now restrict to the case that L(n; m) is homogeneous; as previously mentioned, we can (and will) assume in what follows that m = 1. In this section we derive an analytic description of the distributions of distances on all the L(n; 1) lens spaces.

As a first step to understanding these distributions of distances, we will compute the kth moment of distance between 2 random points in L(n; 1). We now work in join coordinates (2), and we think of points in L(n; 1) as orbits of points in \mathbb{S}^3 . Since L(n; 1) is homogeneous, we may fix one point to be (the orbit of) the point q = (1, 0, 0, 0). The fundamental domain of the Z_n action centered at this point (depicted in Figure 1) is determined by the join coordinate inequalities

$$-\frac{\pi}{n} \le \theta_1, \theta_2 < \frac{\pi}{n},$$

so computing the expectation of kth power of distance in L(n;1) is equivalent to computing the expectation of $[d_{\mathbb{S}^3}(p,q)]^k$, where p varies over this fundamental domain. With p written in join coordinates, $d_{\mathbb{S}^3}(p,q) = \arccos(p \cdot q) = \arccos(\cos \theta_1 \cos \eta)$, so the kth moment of distance is exactly

$$I_{n,k} := \mathbb{E}[d^k; L(n;1)] = \frac{1}{\text{Vol}(L(n;1))} \int_{L(n;1)} [d_{L(n;1)}([p], [q])]^k \, d\text{Vol}_{L(n;1)}$$
$$= \frac{n^2}{2\pi^2} \int_{-\pi/n}^{\pi/n} \int_{-\pi/n}^{\pi/n} \int_0^{\pi/2} \arccos^k(\cos\theta_1 \cos\eta) \cos\eta \sin\eta \, d\eta \, d\theta_1 \, d\theta_2.$$

Obviously,

$$I_{n,0} = 1. (3)$$

For $k \geq 1$, the integral expression for $I_{n,k}$ can be simplified somewhat by integrating out θ_2 , observing that the integrand is even in θ_1 , and making the substitution $\cos u = \cos \theta_1 \cos \eta$. Doing so produces the integral

$$I_{n,k} = \frac{2n}{\pi} \int_0^{\pi/n} \sec^2 \theta_1 \int_{\theta_1}^{\pi/2} u^k \cos u \sin u \, \mathrm{d}u \, \mathrm{d}\theta_1. \tag{4}$$

Notice that this integral is improper for n = 2. For $n \ge 3$ we can apply the reduction formula [13, 2.631.1] for the inner integral to compute the first moment

$$I_{n,1} = \frac{\pi}{2n} + \frac{n-2}{4} \tan \frac{\pi}{n} \tag{5}$$

and the relation

$$I_{n,k} = -\frac{k(k-1)}{4} I_{n,k-2} + \frac{1}{k+1} \left(\frac{\pi}{n}\right)^k + \frac{n}{2\pi} \left[\left(\frac{\pi}{2}\right)^k - \left(\frac{\pi}{n}\right)^k \right] \tan \frac{\pi}{n}$$
 (6)

for $k \geq 2$.

We can solve this recurrence using standard methods. The following theorem expresses the solution in terms of generalized hypergeometric functions ${}_{p}F_{q}\begin{bmatrix} a_{1} & a_{2} & \dots & a_{p} \\ b_{1} & b_{2} & \dots & b_{q} \end{bmatrix}$. In the definition of this class of functions, it is convenient to introduce the *Pochhammer symbol* $(a)_{n}$, defined by the rule

$$(a)_n = \begin{cases} 1 & \text{if } n = 0 \\ a(a+1)\cdots(a+n-1) & \text{if } n \ge 1. \end{cases}$$

Equivalently, so long as a is not a nonpositive integer $(a)_n = \frac{\Gamma(a+n)}{\Gamma(a)}$

In terms of the Pochhammer symbol, the generalized hypergeometric function is defined by the series

$$_{p}F_{q}\begin{bmatrix} a_{1} & a_{2} & \dots & a_{p} \\ b_{1} & b_{2} & \dots & b_{q} \end{bmatrix} = \sum_{n=0}^{\infty} \frac{(a_{1})_{n}(a_{2})_{n} \cdots (a_{p})_{n}}{(b_{1})_{n}(b_{2})_{n} \cdots (b_{q})_{n}} \frac{z^{n}}{n!},$$

provided none of the b_1, \ldots, b_q is a nonpositive integer. When $p \leq q$, the series converges for all z and ${}_pF_q$ is entire.

Theorem 1. For each $k \ge 0$ and each $n \ge 3$, the kth moment of distance on L(n; 1) is

$$I_{n,k} = \frac{1}{(k+1)(k+2)} \left[\frac{4}{k+3} \left(\frac{\pi}{n} \right)^{k+2} {}_{1}F_{2} \left[\frac{1}{\frac{k+4}{2}, \frac{k+5}{2}}; -\frac{\pi^{2}}{n^{2}} \right] + \tan \frac{\pi}{n} \left(n \left(\frac{\pi}{2} \right)^{k+1} {}_{1}F_{2} \left[\frac{1}{\frac{k+3}{2}, \frac{k+4}{2}}; -\frac{\pi^{2}}{4} \right] - 2 \left(\frac{\pi}{n} \right)^{k+1} {}_{1}F_{2} \left[\frac{1}{\frac{k+3}{2}, \frac{k+4}{2}}; -\frac{\pi^{2}}{n^{2}} \right] \right) \right].$$
 (7)

Values for small k are given in Table 1.

Proof. While the difference equation (6) is second-order, the even and odd $I_{n,k}$ are independent of each other, so we can separately reduce each to a first-order difference equation and then solve that first-order equation.

For example, if k = 2m is even, then defining $y_m := I_{n,2m}$ and index-shifting allows us to re-write (6) as

$$y_{m+1} = -\frac{(2m+2)(2m+1)}{4}y_m + \frac{1}{2m+3}\left(\frac{\pi}{n}\right)^{2m+2} + \frac{n}{2\pi}\left[\left(\frac{\pi}{2}\right)^{2m+2} - \left(\frac{\pi}{n}\right)^{2m+2}\right]\tan\frac{\pi}{n}$$

Table 1: Values of the kth moment of distance $I_{n,k}$ for small k and $n \geq 3$.

with initial condition $y_0 = I_{n,0} = 1$ from (3).

This is in the standard form $y_{m+1} = g_m y_m + h_m$ for general first-order linear difference equations, and hence has solution

$$y_{m} = \prod_{j=0}^{m-1} g_{j} \left(y_{0} + \sum_{j=0}^{m-1} \frac{h_{j}}{\prod_{\ell=0}^{j} g_{\ell}} \right)$$

$$= (-1)^{m} \frac{(2m)!}{2^{2m}} \left(1 + \sum_{j=0}^{m-1} \frac{(-1)^{j+1}}{(2j+3)!} \left(\frac{2\pi}{n} \right)^{2j+2} + \frac{n}{2\pi} \tan \frac{\pi}{n} \sum_{j=0}^{m-1} \frac{(-1)^{j+1}}{(2j+2)!} \left(\pi^{2j+2} - \left(\frac{2\pi}{n} \right)^{2j+2} \right) \right)$$

$$(8)$$

after some simplification.

In turn, each of the finite sums becomes one of the hypergeometric functions in (7). For example,

$$1 + \sum_{j=0}^{m-1} \frac{(-1)^{j+1}}{(2j+3)!} \left(\frac{2\pi}{n}\right)^{2j+2} = \frac{n}{2\pi} \sum_{j=0}^{m} \frac{(-1)^{j}}{(2j+1)!} \left(\frac{2\pi}{n}\right)^{2j+1}$$

$$= \frac{n}{2\pi} \sum_{j=0}^{\infty} \frac{(-1)^{j}}{(2j+1)!} \left(\frac{2\pi}{n}\right)^{2j+1} - \frac{n}{2\pi} \sum_{j=m+1}^{\infty} \frac{(-1)^{j}}{(2j+1)!} \left(\frac{2\pi}{n}\right)^{2j+1}$$

$$= \frac{n}{2\pi} \sin \frac{2\pi}{n} - \frac{(-1)^{m+1}}{(2m+3)!} \left(\frac{2\pi}{n}\right)^{2m+2} \sum_{j=0}^{\infty} \frac{1}{(m+2)_{i}(m+\frac{5}{2})_{i}} \left(-\frac{\pi^{2}}{n^{2}}\right)^{i}.$$

After multiplying each term by $1 = \frac{i!}{i!} = \frac{(1)_i}{i!}$, the remaining sum is the standard power series representation of ${}_1F_2\left[\begin{smallmatrix} 1\\ m+2 \end{smallmatrix}\right]_{m+\frac{5}{2}}^{m+\frac{5}{2}}; -\frac{\pi^2}{n^2}$.

Simplifying the remaining terms in (8) and replacing 2m with k yields the solution (7) for the even moments.

On the other hand, notice that we can solve the difference equation (6) for $I_{n,1}$ independent of the value of $I_{n,-1}$. Therefore, if we define $z_m = I_{n,2m-1}$ for $m \ge 1$, we can choose the initial condition z_0 arbitrarily. If we choose $z_0 = 1$, then the difference equation and initial condition for z_m are essentially identical to those in the problem we just solved. Indeed, solving the system and plugging in k = 2m - 1 at the end yields the exact same expression (7) for the odd moments, completing the proof.

We can't plug n=2 into the expressions (5) and (6), but taking the limit as $n\to 2$ gives the corresponding values of the improper integral (4):

$$I_{2,1} = \frac{1}{\pi} + \frac{\pi}{4}$$

$$I_{2,k} = -\frac{k(k-1)}{4}I_{2,k-2} + \frac{1}{k+1}\left(\frac{\pi}{2}\right)^k + \frac{k}{\pi}\left(\frac{\pi}{2}\right)^{k-1}.$$

The solution of this initial value problem (together with $I_{2,0}=1$) is simply the limit of (7) as $n \to 2$:

Corollary 5. The kth moment of distance on $L(2;1) = \mathbb{RP}^3$ is

$$I_{2,k} = \frac{1}{k+1} \left(\frac{\pi}{2}\right)^k \left[2 \,_1F_2 \left[\frac{1}{\frac{k+3}{2}, \frac{k+4}{2}}; -\frac{\pi^2}{4}\right] + \frac{\pi^2}{(k+2)(k+3)} \left(_1F_2 \left[\frac{1}{\frac{k+4}{2}, \frac{k+5}{2}}; -\frac{\pi^2}{4}\right] - \frac{4}{k+4} \,_1F_2 \left[\frac{2}{\frac{k+5}{2}, \frac{k+6}{2}}; -\frac{\pi^2}{4}\right]\right)\right].$$

We point out that the partially oriented flag manifolds $F\ell((1,1,1);\{\{1\},\{2\},\{3\}\})$ and $F\ell((1,1,1),\{\{1\},\{2,3\}\})$ considered in our previous paper [4] are (up to a global scale factor of 2) the lens spaces L(2;1) and L(4;1), respectively, and indeed the expected values of distance that we computed on those spaces were exactly $2I_{2,1} = \frac{2}{\pi} + \frac{\pi}{2}$ and $2I_{4,1} = 1 + \frac{\pi}{4}$.

For small k the finite sum formula (8) is typically more useful than (7)—and, indeed, the finite sum is what we see in Table 1—but one virtue of Theorem 1 and Corollary 5 is that we can easily determine the asymptotic behavior of $I_{n,k}$ as $k \to \infty$ by retaining only the leading terms in the power series representations of the hypergeometric functions.

Corollary 2. For fixed $n \geq 3$, the asymptotic growth of the kth moment of distance on L(n;1) as $k \to \infty$ is

$$I_{n,k} \sim \frac{n}{k^2} \left(\frac{\pi}{2}\right)^{k+1} \tan \frac{\pi}{n}.$$

$$I_{n,-1} = \frac{n}{\pi} \left[\gamma - \operatorname{Ci}\left(\frac{2\pi}{n}\right) + \log\left(\frac{2\pi}{n}\right) + \left(\operatorname{Si}(\pi) - \operatorname{Si}\left(\frac{2\pi}{n}\right)\right) \tan\frac{\pi}{n} \right],$$

where $\gamma \approx 0.577$ is the Euler–Mascheroni constant and Ci and Si are the cosine integral and sine integral functions, respectively.

¹We emphasize that $I_{n,-1} \neq 1$; in fact, it is not too hard to show that

$$k \quad \lim_{n \to \infty} I_{n,k}$$

$$0 \quad 1$$

$$1 \quad \frac{1}{4}\pi$$

$$2 \quad -\frac{1}{2} + \frac{\pi}{8}\pi$$

$$3 \quad \frac{\pi^2 - 6}{16}\pi$$

$$4 \quad \frac{3}{2} + \frac{\pi^3 - 12\pi}{32}\pi$$

$$5 \quad \frac{\pi^4 - 20\pi^2 + 120}{64}\pi$$

$$6 \quad -\frac{45}{4} + \frac{\pi^5 - 30\pi^3 + 360\pi}{128}\pi$$

$$7 \quad \frac{\pi^6 - 42\pi^4 + 840\pi^2 - 5040}{256}\pi$$

Table 2: $\lim_{n\to\infty} I_{n,k}$ for small k. The coefficient of π is the coefficient of $n \tan \frac{\pi}{n}$ in the corresponding entry in Table 1, and the remaining term is the constant term from Table 1.

For n=2, the asymptotic growth of the kth moment of distance on $L(2;1)=\mathbb{RP}^3$ is

$$I_{2,k} \sim \frac{2}{k} \left(\frac{\pi}{2}\right)^k$$
.

On the other hand, if we fix k and let n get large, only the middle term in (7) survives: Corollary 6. For fixed $k \geq 0$,

$$\lim_{n \to \infty} I_{n,k} = \frac{\pi}{(k+2)(k+1)} \left(\frac{\pi}{2}\right)^{k+1} F_2 \left[\frac{1}{\frac{k+3}{2}} \frac{k+4}{2}; -\frac{\pi^2}{4}\right].$$

Values for small k are given in Table 2.

Another way to package the information contained in Theorem 1 is by computing the moment-generating function of distance:

Theorem 3. For $n \geq 3$, the moment-generating function of distance on L(n;1) is

$$M_n(t) = \frac{2n}{\pi(4+t^2)} \left(\frac{2(e^{t\pi/n} - 1)}{t} + \tan\frac{\pi}{n} \left(e^{t\pi/2} - e^{t\pi/n} \right) \right). \tag{9}$$

For n = 2, the moment-generating function is

$$M_2(t) = \frac{4}{\pi(4+t^2)} \left(\frac{2(e^{t\pi/2}-1)}{t} + te^{t\pi/2} \right).$$

Proof. By definition,

$$M_n(t) = \mathbb{E}(e^{td}; L(n; 1)) = \frac{2n}{\pi} \int_0^{\pi/n} \sec^2 \theta_1 \int_{\theta_1}^{\pi/2} e^{tu} \cos u \sin u \, du \, d\theta_1$$
 (10)

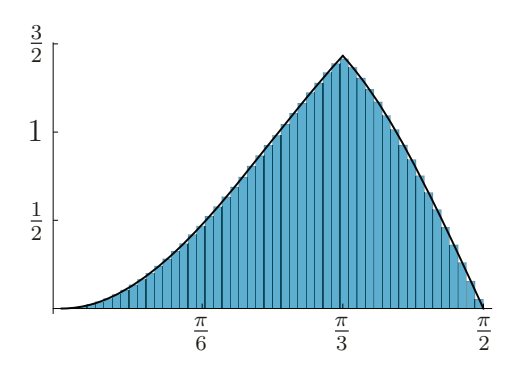


Figure 3: Histogram of distances between 10,000,000 random points on L(3;1) generated by Algorithm 3 compared to the pdf $f_3(x) = \frac{6}{\pi} \left(\sin^2 x + \Theta(x - \pi/3) \left(-\sin^2 x + \sqrt{3}\sin x \cos x \right) \right)$.

using the same substitution that produced (4). Using the identity $\sin 2u = 2 \sin u \cos u$ and integrating by parts twice yields

$$M_n(t) = \frac{2n}{\pi(4+t^2)} \left(\frac{e^{t\pi/n} - 1}{t} + \tan\frac{\pi}{n} e^{t\pi/2} - \int_0^{\pi/n} e^{t\theta_1} (t \tan\theta_1 + \sec^2\theta_1 - 1) d\theta_1 \right)$$

for $n \geq 3$. Integrating the first term inside the integral by parts produces a term which cancels the second, and the rest is straightforward.

For n = 2, evaluating the indefinite integral (10) boils down to taking the limit of (9) as $n \to 2$, which produces the desired expression for $M_2(t)$.

We can recover the probability density function (pdf) f_n of distance as the inverse Laplace transform of $M_n(-t)$:

$$f_2(x) = \frac{4}{\pi} \sin^2 x$$

$$f_n(x) = \frac{2n}{\pi} \left(\sin^2 x + \Theta(x - \pi/n) \left(-\sin^2 x + \sin x \cos x \tan \frac{\pi}{n} \right) \right), \tag{11}$$

where Θ is the Heaviside function which is zero for negative values and 1 for positive values. See Figure 3.

As $n \to \infty$ we see that $f_n(x) \to \sin 2x$, the pdf of the *sine distribution* introduced by Gilbert in the study of moon craters [11, 12]. It is not so surprising to see this distribution: as $n \to \infty$ the lens spaces L(n; 1) converge in the Gromov–Hausdorff sense to a 2-sphere of radius 1/2, and the distance distribution on this sphere is exactly the sine distribution.

In turn, given the pdf, we can integrate to get the cumulative distribution function $F_n(x)$ of distance on L(n; 1):

$$F_2(x) = \frac{2}{\pi} (x - \sin x \cos x)$$

$$F_n(x) = \frac{n}{\pi} \left(x - \sin x \cos x + \Theta(x - \pi/n) \left(\frac{\pi}{n} - x + \sin x \cos x - \cos^2 x \tan \frac{\pi}{n} \right) \right);$$

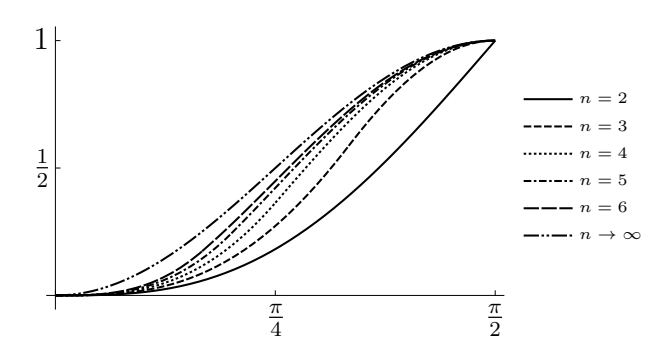


Figure 4: The cumulative distribution function of distance on L(n;1) for $2 \le n \le 6$ and in the limit as $n \to \infty$.

see Figure 4.

By definition,

$$F_n(x) = \mathbb{P}(d(p,q) \le x) = \frac{\operatorname{Vol} B_q(x)}{\operatorname{Vol} L(n;1)}$$

where $q \in L(n; 1)$ is any fixed point and $p \in L(n; 1)$ is random; since L(n; 1) is homogeneous this is independent of q. Hence, we can compute the volume $V_n(r) := \text{Vol } B_q(r)$ of a ball of radius r in L(n; 1) as

$$V_n(r) = \text{Vol}(L(n; 1))F_n(r) = \frac{2\pi^2}{n}F_n(r).$$

This proves:

Theorem 4. For $n \geq 2$, the volume of a ball of radius r in L(n; 1) is

$$V_n(r) = \begin{cases} 2\pi(r - \sin r \cos r) & \text{if } r \le \frac{\pi}{n} \\ \frac{2\pi^2}{n} - 2\pi \cos^2 r \tan \frac{\pi}{n} & \text{else.} \end{cases}$$

Since the diameter of L(n; 1) is $\frac{\pi}{2}$, V_n is only defined on $[0, \frac{\pi}{2}]$, so we never reach the second case when n = 2. Also, $2\pi(r - \sin r \cos r)$ is simply the volume of a ball of radius r in \mathbb{S}^3 ; not surprisingly, things get interesting only when $r > \frac{\pi}{n}$, the injectivity radius of L(n; 1).

Thinking in these geometric terms, the pdfs from (11) are scaled areas of spheres. Rescaling by the same $\frac{2\pi^2}{n}$ factor as above yields the surface area $A_n(r)$ of the sphere of radius r centered at any point in L(n;1):

$$A_n(r) = \begin{cases} 4\pi \sin^2 r & \text{if } r \leq \frac{\pi}{n} \\ 4\pi \sin r \cos r \tan \frac{\pi}{n} & \text{else.} \end{cases}$$

5 Concluding Remarks

Three-dimensional lens spaces are a family of topological/geometric objects that have played a historical role in the development of manifold theory. Their interest derives both from

their ease of construction and as examples of manifolds exhibiting unusual phenomena. They appear across several disciplines including topology, geometry, cosmography, and data science, and are a natural setting for spherical data with cyclic symmetries. While lens spaces have been well studied from varying perspectives, we are unaware of other sources which consider distance distributions on them.

Distance distributions have been used in geometric classification and can be used to understand general metric measure spaces. While they can often be approximated effectively using Monte Carlo techniques, it would be interesting to determine analytic expressions for distance distributions on a broader class of manifolds. For manifolds which are not homogeneous spaces, the distribution of distances from a fixed point depends on the point. In other words, the volume formula for a ball is dependent on the location of the center of the ball in the manifold. In turn, integrating the distribution of distances from a fixed point as the fixed point varies over the manifold yields the distribution of distances between pairs of random points.

Non-homogeneous lens spaces, both in three and in higher dimensions, are particularly tractable examples of non-homogeneous manifolds, so in these spaces it may be feasible to find analytic expressions for the distributions of distances both from a fixed point and between random points.

Acknowledgments

We thank all the participants in the Pattern Analysis Lab at Colorado State University for their energy, ideas, and ongoing inspiration, Tom Needham for helpful conversations, and the National Science Foundation (CCF–BSF:CIF #1712788, ATD #1830676, CP) and the Simons Foundation (#354225, CS) for their support.

References

- [1] Luis Alday, Martin Fluder, and James Sparks. The large N limit of M2-branes on lens spaces. Journal of High Energy Physics, 2012:57, 2012.
- [2] James Waddell Alexander. Note on two three-dimensional manifolds with the same group. Transactions of the American Mathematical Society, 20(4):339–342, 1919.
- [3] Ralf Aurich and Sven Lustig. A survey of lens spaces and large-scale cosmic microwave background anisotropy. *Monthly Notices of the Royal Astronomical Society*, 424(2):1556–1562, 2012.
- [4] Brenden Balch, Chris Peterson, and Clayton Shonkwiler. Expected distances on manifolds of partially oriented flags. Preprint, 2020, arXiv:2001.07854 [math.DG].

- [5] José R. Berrendero, Antonio Cuevas, and Beatriz Pateiro-López. Shape classification based on interpoint distance distributions. *Journal of Multivariate Analysis*, 146:237–247, 2016.
- [6] Marco Bonetti and Marcello Pagano. The interpoint distance distribution as a descriptor of point patterns, with an application to spatial disease clustering. *Statistics in Medicine*, 24(5):753–773, 2005.
- [7] Mireille Boutin and Gregor Kemper. On reconstructing n-point configurations from the distribution of distances or areas. Advances in Applied Mathematics, 32(4):709–735, 2004.
- [8] Daniel Brinkman and Peter J. Olver. Invariant histograms. *The American Mathematical Monthly*, 119(1):4–24, 2012.
- [9] Elmer Julian Brody. The topological classification of the lens spaces. Annals of Mathematics, Second Series, 71(1):163–184, 1960.
- [10] Alan Edelman, Tomás A. Arias, and Steven T. Smith. The geometry of algorithms with orthogonality constraints. SIAM Journal on Matrix Analysis and Applications, 20(2):303–353, 1998.
- [11] Anthony William Fairbank Edwards. Gilbert's sine distribution. *Teaching Statistics*, 22(3):70–71, 2000.
- [12] Grove Karl Gilbert. The moon's face: A study of the origin of its features. Bulletin of the Philosophical Society of Washington, 12:241–292, 1893.
- [13] Izrail S. Gradshteyn and Iosif M. Ryzhik. *Table of Integrals, Series, and Products*. Elsevier, Amsterdam, eighth edition, 2015.
- [14] Alfred Gray and Lieven Vanhecke. Riemannian geometry as determined by the volumes of small geodesic balls. *Acta Mathematica*, 142(3–4):157–198, 1979.
- [15] Akira Ikeda and Yoshihiko Yamamoto. On the spectra of 3-dimensional lens spaces. Osaka Journal of Mathematics, 16(2):447–469, 1979.
- [16] Roland Lehoucq, Jean-Philippe Uzan, and Jeffrey Weeks. Eigenmodes of lens and prism spaces. *Kodai Mathematical Journal*, 26(1):119–136, 2003.
- [17] Facundo Mémoli. Gromov-Wasserstein distances and the metric approach to object matching. Foundations of Computational Mathematics, 11(4):417–487, 2011.
- [18] Facundo Mémoli and Tom Needham. Gromov-Monge quasi-metrics and distance distributions. Preprint, 2018, arXiv:1810.09646 [math.MG].
- [19] Robert Osada, Thomas Funkhouser, Bernard Chazelle, and David Dobkin. Shape distributions. *ACM Transactions on Graphics*, 21(4):807–832, 2002.

- [20] Luis Polanco and Jose A. Perea. Coordinatizing data with lens spaces and persistent cohomology. In Zachary Friggstad and Jean-Lou De Carufel, editors, *Proceedings of the 31st Canadian Conference on Computational Geometry (CCCG 2019)*, pages 49–58, 2019.
- [21] Józef H. Przytycki and Akira Yasukhara. Symmetry of links and classification of lens spaces. Geometriae Dedicata, 98(1):5–61, 2003.
- [22] Kurt Reidemeister. Homotopieringe und Linsenräume. Abhandlungen aus dem Mathematischen Seminar der Universität Hamburg, 11(1):102–109, 1935.
- [23] Paolo Salvatore and Riccardo Longoni. Configuration spaces are not homotopy invariant. *Topology*, 44(2):375–380, 2005.
- [24] Minoru Tanaka. Compact Riemannian manifolds which are isospectral to threedimensional lens spaces. II. Proceedings of the Faculty of Science of Tokai University, 14:11–34, 1979.
- [25] Heinrich Tietze. Über die topologischen Invarianten mehrdimensionaler Mannigfaltigkeiten. Monatshefte für Mathematik und Physik, 19:1–118, 1908.
- [26] Shinya Tomizawa. Multicharged black lens. Physical Review D, 100(2):024056, 2019.
- [27] Jean-Philippe Uzan, Alain Riazuelo, Roland Lehoucq, and Jeffrey Weeks. Cosmic microwave background constraints on lens spaces. *Physical Review D*, 69(4):043003, 2004.
- [28] Celso Viana. The isoperimetric problem for lens spaces. *Mathematische Annalen*, 374(1):475–497, 2018.
- [29] Joseph A. Wolf. *Spaces of Constant Curvature*. AMS Chelsea Publishing, Providence, RI, sixth edition, 2011.